Detecting Broken Rotor Bars in Induction Motors with Model-Based Support Vector Classifiers

Mohammed Obaid Mustafa, Damiano Varagnolo, George Nikolakopoulos, and Thomas Gustafsson

***Abstract*—We propose a methodology for testing the sanity of motors when both healthy and faulty data are unavailable. More precisely, we consider a model-based Support Vector Classification (SVC) method for the detection of broken bars in three phase asynchronous motors at full load conditions, using features based on the spectral analysis of the stator's steady state current (more specifically, the amplitude of the lift sideband harmonic and the amplitude at fundamental frequency). We diverge from the mainstream focus on using SVCs trained from measured data, and instead derive a classifier that is constructed entirely using theoretical considerations. The advantage of this approach is that it does not need training steps (an expensive, time consuming and often practically infeasible task), i.e., operators are not required to have both healthy and faulty data from a system for checking it. We describe what are the theoretical properties and fundamental limitations of using model based SVC methodologies, provide conditions under which using SVC tests is statistically optimal, and present some experimental results to prove the effectiveness of the suggested scheme.**

***Index Terms*—fault detection, model based methods, broken rotor bar, three phase asynchronous motors, statistical characterization, Support Vector Classification, Motor Current Signature Analysis.**

I. Introduction

The interests in the on-line Fault Detection and Diagnosis (FDD) of faults in induction motors is given by the fact that more than 80% of industrial electromechanical converters are Induction Motors (IMs) [1]. Despite being highly reliable, these electromechanical devices are also subject to many types of faults. Early detection is then crucial to reduce maintenance costs, prevent unscheduled downtimes for electrical drive systems, and prevent risks for humans.

Among the various possible faults in IMs, most of them occur in their rotor and/or stator. The most common faults are openings or shortings of one or more of the stator's phase windings [2], broken rotor bars or cracked rotor's end-rings [3], static or dynamic air–gap irregularities [4], and bearing failures [5].

Many faults appear gradually, and sometimes it can be very difficult to detect them before they induce faults in connected processes. To ease the detection of these faults, a variety of sensors can be used to collect meaningful information. The most common sensors are measurements of stator voltages and currents [4], external magnetic flux densities [6], rotor position and speed [7], output torque [7], internal and external temperatures [8], and vibrations [9].

M. O. Mustafa, D. Vargnolo, G. Nikolakopoulos, and T. Gustafsson are with the Division of Signals and Systems, Department of Computer Science, Electrical and Space Engineering, Luleå University of Technology, Luleå, Sweden. Email: { mohammed.obaid | damiano.varagnolo | george.nikolakopoulos | thomas.gustafsson }.@ltu.se.

The main objective of on-line FDD schemes is to detect and isolate the fault in its early stages. The aim of this manuscript is then to develop and analyze a model-based scheme for the detection of broken bars in IMs.

Literature review: FDD schemes aim at distinguishing potential failure conditions from normal operating ones [10]. The main dichotomy separates the existing schemes in:

model-based methods: here one first determines analytically mathematical models from first-principles, and then checks if the information obtained from measurements comply with these models or not [15]. The advantages of these methods are that they do not need observations from both fault-free and faulty systems (that might not be available) and can thus be implemented in already existing plants;

model-free methods: here one gets measurements from a fault-free, a faulty and a to-be checked motors, and then decides whether the motor is healthy or faulty considering if the to-be checked measurements are (statistically) closer to the fault-free or the faulty ones. The advantages of these methods are that they potentially do not suffer of imprecisions in the theoretical models describing the motor (due, e.g., to simplifications, construction tolerances and wear of the machine). Disadvantages of model-free methods are in the difficulty of obtaining data and in the absence of generalization capabilities: indeed training a method using a specific motor does not guarantee that that method will work for other motors.

As stated more precisely in the statement of contributions, our method exploits a model-based strategy that uses Support Vector Classifications (SVCs) and evaluations of the sidebands of the harmonics of the stator current (also known as Motor Current Signature Analysis (MCSA)). In the next bulleted paragraphs we thus review literature on model-based methods, literature on model-free methods based on SVC strategies, and literature on model-free methods exploiting properties of the stator current.

- Model-based methods: among the few manuscripts in this category, [16] performs fault detection and localization of stator and rotor faults in IMs using model structures that are derived from theoretical considerations as in this manuscript, but using parametric estimation methods instead of SVC strategies. Also [17] develops an empirical model-based fault diagnosis system, but using recurrent dynamic Neural Networks and multi-resolution signal processing methods, and lacks describing the theoretical properties of the strategy. [12] exploits instead models obtained using finite-element methods, and thus techniques and software tools not always available to practitioners.

• Model-free methods based on SVC strategies: Support Vector Classifications are based on structural risk minimization concepts [18], and require selecting opportune *features*, i.e., measurable and quantifiable characteristics to be exploited as benchmarks (see Section VIII for more details). In literature one can find reviews on the generic usage of SVC technologies for the monitoring of machine conditions and for the diagnosis of faults [19]. Other works instead deal specifically with motors. E.g., [20] tests unbalance, misalignment and mechanical looseness in three phase induction motors using measurements of vibrations as features. [21] instead detects broken bars by using features that are based on discrete wavelet transforms and wavelet packet transforms of the motor current signatures (the benefit of using these transforms being to require lower sampling rates). [22] also uses spectral information of the phase current and phase voltage.

• Model-free methods based on properties of the stator current: broken bars introduce distortions in the air-gap field that eventually modify the envelope and the spectrum of the current. Faulty spectra have indeed specific sideband components around the main supply frequency; FDD schemes can then act by checking the presence of these specific frequency components [23], [24], [25], [26], [13]. One can also exploit analysis of the envelope of the current, since faults cause modulation effects in time that are not present in non-faulty conditions. For example, [27] analyzes these envelopes using Gaussian mixture models and reconstructed phase spaces to identify motor faults. On the other hand MCSA is the optimal choice for electrical machines under steady-state conditions and rated load [1], while frequency analysis is a generally exploited concept for checking industrial equipment [11].

Statement of contributions: We propose a model-based SVC technique: more specifically, we construct SVCs starting from features computed from models of fault-free and faulty motors. In this way we therefore do not need collecting training datasets, and thus address the situation in which there is no possibility of collecting data from both fault-free and faulty systems.

The selected features are the ones that are currently believed to be the most powerful ones for motor fault classification purposes, i.e., features based on the analysis of the spectrum of the stator current at full load conditions. Remarkably, even if we explicitly derive the technique for these specific features, we also provide and discuss a general framework that can be used also for other features. We are thus proposing a methodology rather than simply a method.

We then also answer the question of why one should use a SVC strategy, motivate under which assumptions it is statistically correct to use SVC approaches, and perform experimental evaluations on real case scenarios to prove the validity of the technique for practical purposes.

At the best of our knowledge, thus, our contributions w.r.t. to the existing literature are: *i)* we propose for the first time and validate against real data a model-based SVC technique; *ii)* we propose a broad methodology that can be applied to generic features; *iii)* we clarify under which assumptions it is statistically optimal to use SVC strategies.

Organization of the manuscript: Section II starts with describing the effects of broken bars in IMs. Section III then introduces in general terms our methodology. Sections from IV to XI detail the specific steps defined by our methodology. Section XI reports also a statistical analysis of the proposed classification rule. Section XII describes some numerical results on artificially broken IMs. Section XIII then concludes by summarizing some remarks on the findings and by outlining future development lines.

II. Effects of broken bars on Induction Motors

Rotor bars break because of thermal, magnetic, residual, dynamic, and mechanical stresses [2], [23], and constitute a significant part of the problems in induction motors [28], [29].

According to the generalized rotating field theory [30], healthy motors have symmetrical stator windings that produce a field that is rotating at the supply frequency f_s; this induces an Electro-Magnetic Field (EMF) in the rotor circuits rotating at frequency sf_s, where s is the slip.

Broken rotor bars cause asymmetries in the resistance and in the inductance of the rotor's phases, that then generate asymmetries in the rotating electromagnetic field in the air gap between stator and rotor. Consequently, broken rotor bars produce back-ward rotating field and additional non-sinusoidal EMF components that induce frequency harmonics in the stator current [24]. More specifically, changes are specially in the amplitude of the sidebands [9], [23]

$$(1 \mp 2ks)f_s, \qquad k = 1, 2, \ldots. \tag{1}$$

Thus the spectrum of the stator currents contains information useful for detecting faults, since the frequency spectra of faulty and healthy motors differentiate in the sidebands, with a magnitude of these variations that is also dependent on the severity of the fault [24].

III. Model-Based Support Vector Classification: Methodology

Figure 1 summarizes the quantities involved in our methodology. More precisely:

- $v_s^m(t)$ is the measured signal of the stator voltages, and represents the input of the motor. It is a *directly measured quantity* returned by the measurement system;
- P is the real motor, i.e., the physical device;
- P^h and P^f are mathematical models of P under healthy (h) or faulty (f) assumptions. They are *directly computed quantities* derived from first principles. They thus do not depend on any of the other quantities summarized in Figure 1 rather than the nominal parameters of P;
- $i_s^m(t)$ is the measured stator currents, and represents the output of the motor.
- $i_s^h(t)$ and $i_s^f(t)$ are the stator currents obtained driving the theoretical models P^h and P^f with the measured input $v_s^m(t)$. They are *indirectly computed quantities*, and depend only on the measured signal $v_s^m(t)$ and the models P^h and P^f;

- $\Phi(\cdot)$ maps stator currents ($i_s^m(t)$, $i_s^h(t)$, or $i_s^f(t)$) into a point in the features space. Formally, thus,

$$\boldsymbol{\phi}^* = \Phi\left(i_s^\star(t)\right) \text{ where } * \in \{m, h, f\}. \tag{2}$$

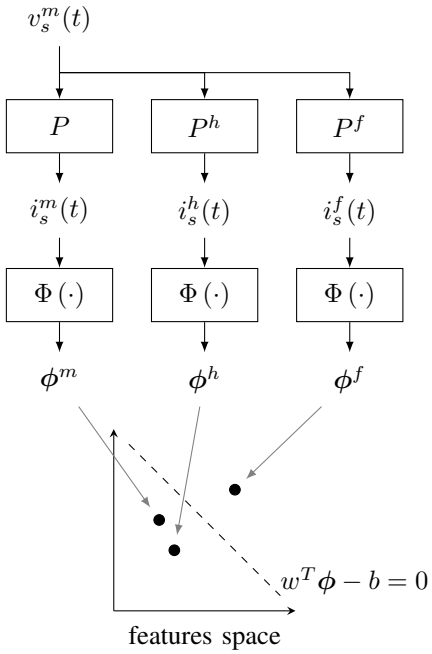

Figure 1. Summary of the quantities involved in our considerations.

We propose the following model-based SVC methodology, where the execution of steps Step-1 to Step-5 are performed a priori, before receiving the measurements:

Step-1: construct P^h and P^f from the specifics of the motor P;
Step-2: compute, by means of P^h and P^f, the currents $i_s^h(t)$ and $i_s^f(t)$;
Step-3: define the currents-to-features map Φ;
Step-4: compute, by means of the map Φ, the features $\boldsymbol{\phi}^h$ and $\boldsymbol{\phi}^f$;
Step-5: build from $\boldsymbol{\phi}^h$ and $\boldsymbol{\phi}^f$ the corresponding SVC rule;
Step-6: measure, by means of an opportune Data Acquisition (DAQ) system, the stator voltages $v_s^m(t)$ and currents $i_s^m(t)$;
Step-7: compute, by means of the map Φ, the features $\boldsymbol{\phi}^m$;
Step-8: decide if the motor is in healthy or faulty conditions by classifying $\boldsymbol{\phi}^m$ by means of the constructed SVC.

Each of the following sections describes one of the previous steps. Section XI, in particular, motivates the focus on SVC paradigms, and provides theoretical considerations on the robustness of the method against uncertainties in the measurement system.

IV. Step-1: construct P^h and P^f

A. Construct P^h

Assume that the system is healthy. As proposed in [31], a generic single phase of the induction motor can be represented with the equivalent circuit in Figure 2.

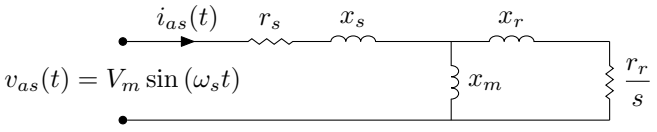

Figure 2. Equivalent representation of a single phase of a general induction motor under healthy assumptions [31].

The parameters r_s, x_s, x_r, x_m, r_r defining the circuit in Figure 2 are computed directly starting from the nominal specifics of the motor. The slip s can instead be computed as

$$s = \frac{N_s - Nr}{N_s} \tag{3}$$

where $N_s = \frac{60 f_s}{p}$, p is the poles pair defining the motor model, and N_r is the rotational speed of the induction motor.

B. Construct P^f

We hypothesize that the faulty conditions are given because of broken bars in the rotor cage so that, as described in Section II, frequency harmonics appear in the stator currents. As in [30], [32], we pose the following assumptions:

Assumption 1 The impact of broken rotor bars is modeled by:
A1) unbalancing the rotor resistance;
A2) neglecting changes in the rotor inductances;
A3) neglecting effects from the end-ring;
A4) neglecting magnetizing currents;
A5) letting broken bars be contiguous;
A6) letting the slip value be near the rated one, so that the rotor effective reactances are small with respect to resistances.

Notice that Assumptions A1 to A4 can be safely posed since their influence is insignificant compared to the changes in the rotor resistance, while Assumption A5 can be safely posed because it describes the typical breakage pattern.

As described in Section II, broken rotor bars induce frequency harmonics in the stator current in the sidebands of the supply frequencies described in (1). In a motor with N bars, n broken bars will thus simply an increment of the phase a's resistance Δr_{ra} equal to [33]

$$\Delta r = r_r \frac{3n}{N - 3n}. \tag{4}$$

V. Step-2: compute $i_s^h(t)$ and $i_s^f(t)$

A. Compute $i_s^h(t)$

Thanks to the representation of P^h given in Figure 2, we can compute the stator current in healthy conditions as

$$i_{as}^h(t) = \frac{v_{as}(t)}{Z_m} = \frac{V_m \sin(2\pi f_s t - \angle Z_m)}{|Z_m|} \tag{5}$$

where Z_m is the equivalent impedance of the circuit, given by

$$Z_m = r_s + jx_s + \left[\frac{\left(\frac{r_r}{s} + jx_r\right)(jx_m)}{\frac{r_r}{s} + j(x_r + x_m)} \right]. \tag{6}$$

B. Compute $i_s^f(t)$

Consider the faulty model P^f analyzed in Section IV-B, and the simplificative assumption (motivated by the discussion in Section IV-B and borrowed from [31], [30]) for which the faulty current signal is given by

$$\begin{cases} i_{as}^f(t) = & I_m \sin\left(2\pi f_s t\right) \\ & +I_l \sin\left(2\pi f_l t - \alpha_l\right) \\ & +I_r \sin\left(2\pi f_r t - \alpha_r\right) & \text{(7a)} \\ i_{bs}^f(t) = & I_m \sin\left(2\pi f_s t - 2\pi/3\right) \\ & +I_l \sin\left(2\pi f_l t - \alpha_l - 2\pi/3\right) \\ & +I_r \sin\left(2\pi f_r t - \alpha_r - 2\pi/3\right) & \text{(7b)} \\ i_{bs}^f(t) = & I_m \sin\left(2\pi f_s t + 2\pi/3\right) \\ & +I_l \sin\left(2\pi f_l t - \alpha_l + 2\pi/3\right) \\ & +I_r \sin\left(2\pi f_r t - \alpha_r + 2\pi/3\right) & \text{(7c)} \end{cases}$$

where

$$\begin{cases} f_l := (1-2s)\, f_s \\ f_r := (1+2s)\, f_s. \end{cases} \tag{8}$$

Practically speaking, by considering (7) we obtain an approximated spectrum that matches the faulty one around the frequencies of interest f_l and f_s (the unique ones considered in our methodology).

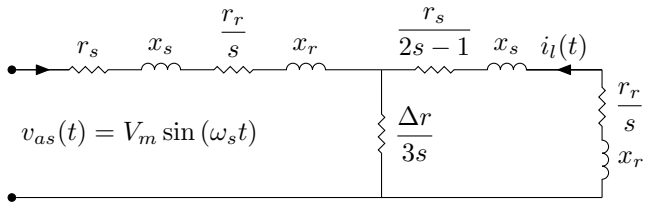

Figure 3. Auxiliary circuit instrumental to compute the amplitude I_l introduced in (7) [31].

Thanks to this approximation the amplitudes I_l and I_r (that are assumed to be equal, as in [23], [30]) can be computed as the maximal amplitude of the sinusoidal signal $i_l(t)$ auxiliary and circuit in Figure 3. We thus remark that the circuit in Figure 3 is not representing the motor: it is an ancillary circuit to compute the amplitudes I_l and I_r. Notice that the angular displacements α_l and α_r can be computed using similar circuits, omitted here for brevity, but available in [30], [34].

VI. Step-3: define $\Phi(\cdot)$

The currents-to-features map $\Phi(\cdot)$ computes the main and left-side harmonics of the stator current. More specifically, the features are computed starting from a generic stator current $i_{as}^\star(t)$, with $\star \in \{m, h, f\}$, and using the following procedure:

1) window the signal $i_{as}^\star(t)$ in $t = [0, T]$, i.e., compute

$$\bar{i}_{as}^\star(t) = \begin{cases} i_{as}^\star(t) & \text{for } t \in [0,T] \\ 0 & \text{otherwise;} \end{cases} \tag{9}$$

2) compute the Fourier Transform (FT) of the windowed current $\bar{i}_{ac}^\star(t)$, i.e., compute

$$\widehat{i}_{as}^\star(f) = \int_{\mathbb{R}} \bar{i}_{as}^\star(t) \exp\left(-2\pi j f t\right) dt; \tag{10}$$

3) compute the features $\boldsymbol{\phi}^*$ as the amplitude of the FT evaluated at the supply frequency f_s and at the frequency f_l defined in (8), i.e., compute

$$\boldsymbol{\phi}^\star = \Phi\left(i_{as}^\star\right) = \begin{bmatrix} \left|\widehat{i}_{as}^\star\left(f_s\right)\right| \\ \left|\widehat{i}_{as}^\star\left(f_l\right)\right| \end{bmatrix}. \tag{11}$$

VII. Step-4: compute $\boldsymbol{\phi}^h$, and $\boldsymbol{\phi}^f$

A. Compute $\boldsymbol{\phi}^h$

Consider $i_{as}^h(t)$ computed in (5). Then the windowed stator current $\bar{i}_{as}^h(t)$, i.e.,

$$\bar{i}_{as}^h(t) = \begin{cases} \dfrac{V_m \sin\left(2\pi f_s t - \angle Z_m\right)}{|Z_m|} & \text{for } t \in [0,T] \\ 0 & \text{otherwise.} \end{cases} \tag{12}$$

is a windowed sinusoidal. This means that its FT $\widehat{i}_{as}^h(f)$,

$$\widehat{i}_{as}^h(f) = \int_{\mathbb{R}} \bar{i}_{as}^h(t) \exp\left(-2\pi j f t\right) dt, \tag{13}$$

is a sinc function centered around the fundamental frequency f_s, i.e.,

$$\widehat{i}_{as}^h(f) = I_m T \frac{\sin\left(\pi T(f - f_s)\right)}{\pi T(f - f_s)}, \qquad I_m = \frac{V_m}{|Z_m|}. \tag{14}$$

This means that

$$\boldsymbol{\phi}^h = \begin{bmatrix} I_m T \dfrac{\sin\left(T\pi f_s\right)}{T\pi f_s} \\ I_m T \dfrac{\sin\left(2T\pi s f_s\right)}{2T\pi s f_s} \end{bmatrix}. \tag{15}$$

B. Compute $\boldsymbol{\phi}^f$

Consider $i_{as}^f(t)$ computed in (7). Then again the windowed stator current $\bar{i}_{as}^f(t)$ is a sum of windowed sinusoidals. This implies that its FT $\widehat{i}_{as}^f(f)$ evaluated at the generic frequency f is the sum of 3 sinc functions centered around the fundamental frequency f_s, i.e.,

$$\begin{aligned} \widehat{i}_{as}^f(f) = \quad & I_m T \frac{\sin\left(\pi T(f - f_s)\right)}{\pi T(f - f_s)} \\ & + I_l T \frac{\sin\left(\pi T(f - f_l)\right)}{\pi T(f - f_l)} \exp\left(-2\pi j f \alpha_l\right) \\ & + I_r T \frac{\sin\left(\pi T(f - f_r)\right)}{\pi T(f - f_r)} \exp\left(-2\pi j f \alpha_r\right). \end{aligned} \tag{16}$$

This means that

$$\boldsymbol{\phi}^f = \begin{bmatrix} I_m T + (I_l T + I_r T)\,\dfrac{\sin\left(2T\pi s f_s\right)}{2T\pi s f_s} \\ I_m T \dfrac{\sin\left(2\pi T s f_s\right)}{2T\pi s f_s} + I_l T + I_r T \dfrac{\sin\left(4T\pi s f_s\right)}{4T\pi s f_s} \end{bmatrix}. \tag{17}$$

VIII. Step-5: build the SVC

Here we aim at building the separating hyperplane $w^T\boldsymbol{\phi} - b = 0$ that is depicted in Figure 1 and that corresponds to our healthy / faulty classification rule. Let then the dataset $\mathcal{D}$ be composed of just the two datapoints $\left(\boldsymbol{\phi}^h, +1\right)$ and $\left(\boldsymbol{\phi}^f, -1\right)$, where the subscript h denotes "healthy" while f denotes "faulty". To derive the equations of the linear hyperplane $w^T\boldsymbol{\phi} - b = 0$ separating $\mathcal{D}$, since the two datapoints will surely be Support Vectors (SVs) we consider the equivalent SVC optimization problem

$$\begin{array}{ll} \arg_{w,b}\min & \frac{1}{2}\left\|w\right\|^2 \\ \text{s.t.} & w^T\boldsymbol{\phi}^h - b = 1 \\ & w^T\boldsymbol{\phi}^f - b = -1. \end{array} \tag{18}$$

The associated Lagrangian is then

$$\begin{array}{rl} \Lambda\left(w, b, \lambda^h, \lambda^f\right) := & \dfrac{1}{2} w^T w \\ & +\lambda^h\left(w^T\boldsymbol{\phi}^h - b - 1\right) \\ & +\lambda^f\left(w^T\boldsymbol{\phi}^f - b + 1\right). \end{array} \tag{19}$$

The optimal values for w and b are then derived from getting Λ's critical points, i.e., from setting

$$\begin{bmatrix} \dfrac{\partial\Lambda}{\partial w} & \dfrac{\partial\Lambda}{\partial b} & \dfrac{\partial\Lambda}{\partial\lambda^h} & \dfrac{\partial\Lambda}{\partial\lambda^f} \end{bmatrix} = \begin{bmatrix} 0 & 0 & 0 & 0 \end{bmatrix}, \tag{20}$$

or, equivalently,

$$\begin{cases} w + \lambda^h\boldsymbol{\phi}^h + \lambda^f\boldsymbol{\phi}^f = 0 \\ \lambda^h + \lambda^f = 0 \\ w^T\boldsymbol{\phi}^h - b - 1 = 0 \\ w^T\boldsymbol{\phi}^f - b + 1 = 0 \end{cases} \tag{21}$$

that, expanded, leads to

$$\begin{cases} \lambda^h = -\lambda^f \\ \lambda^f = \dfrac{2}{\left\|\boldsymbol{\phi}^h - \boldsymbol{\phi}^f\right\|^2} \\ w = \dfrac{2\left(\boldsymbol{\phi}^h - \boldsymbol{\phi}^f\right)}{\left\|\boldsymbol{\phi}^h - \boldsymbol{\phi}^f\right\|^2} \\ b = \dfrac{\left(\boldsymbol{\phi}^h - \boldsymbol{\phi}^f\right)^T\left(\boldsymbol{\phi}^h + \boldsymbol{\phi}^f\right)}{\left\|\boldsymbol{\phi}^h - \boldsymbol{\phi}^f\right\|^2} \end{cases} \tag{22}$$

and a margin of, as expected,

$$m = \frac{2}{\|w\|} = \|\boldsymbol{\phi}^h - \boldsymbol{\phi}^f\|. \tag{23}$$

IX. Step-6: measure $v_s^m(t)$ and $i_s^m(t)$

As for the stator voltages, we assume that $v_{as}^m(t)$, $v_{bs}^m(t)$, and $v_{cs}^m(t)$ are perfectly measured, and that the rotor voltages $v_{ar}^m(t)$, $v_{br}^m(t)$ and $v_{cr}^m(t)$ are zero. The maximum voltage V_m and the supply frequency f_s are also assumed to be perfectly known. We thus assume that we do not need to measure $v_s^m(t)$.

As for the stator currents, we assume that $i_{as}^m(t)$, $i_{bs}^m(t)$, and $i_{cs}^m(t)$ are measured by the DAQ system.

X. Step-7: compute $\boldsymbol{\phi}^m$

Once $i_{as}^m(t)$ is given by the measurement system, $\boldsymbol{\phi}^m$ is computed numerically using the 3 steps (9), (10) and (11) given above.

XI. Step-8: decide whether the motor is faulty or healthy

Recall that at this stage the SVC rule (w, b) has already been constructed from $\boldsymbol{\phi}_h$ and $\boldsymbol{\phi}_f$. $\boldsymbol{\phi}^m$ is then directly mapped into a *healthy / faulty* decision by means of

$$g\left(i_{as}^m\right) := \begin{cases} \mathcal{H}_0 \text{ (healthy)} & \text{if } w^T\boldsymbol{\phi}^m - b > 0 \\ \mathcal{H}_1 \text{ (faulty)} & \text{otherwise.} \end{cases} \tag{24}$$

A. Assess the quality of the decision rule $g(\cdot)$ – Intuitions

Let us postpone formal definitions to the following Section XI-B. We then intuitively consider that our methodology suffers of 3 sources of uncertainty:

1) measurement noise, that is present on $\boldsymbol{\phi}^m$;
2) parameters uncertainties, that are present on $\boldsymbol{\phi}^h$ and $\boldsymbol{\phi}^f$.

These uncertainties then make the decision rule $g(\cdot)$ prone to errors. But how much?

In the following section we analytically address the situation for which only $\boldsymbol{\phi}^m$ is uncertain. Due to space limitations, we postpone addressing uncertainties also on $\boldsymbol{\phi}^h$ and $\boldsymbol{\phi}^f$ in future works, that will focus entirely on robustness and sensitivity issues.

B. Assess the quality of the decision rule $g(\cdot)$ – Formal derivations

Assume that, independently of healthy or faulty conditions, the measured current $i_{as}^h(t)$ is corrupted by a white noise $\delta i(t)$, i.e., that

$$i_{as}^h(t) = \begin{cases} i_{as}^h(t) + \delta i(t) & \text{if } \mathcal{H}_0 \\ i_{as}^f(t) + \delta i(t) & \text{if } \mathcal{H}_1 \end{cases} \tag{25}$$

where $\delta i(t)$ is a (potentially non-Gaussian) white noise with finite variance σ^2. Since the operations in steps 1, 2 and 3 are linear, it follows that

$$\boldsymbol{\phi}^m = \begin{cases} \boldsymbol{\phi}^h + \delta\boldsymbol{\phi} & \text{if } \mathcal{H}_0 \\ \boldsymbol{\phi}^f + \delta\boldsymbol{\phi} & \text{if } \mathcal{H}_1. \end{cases} \tag{26}$$

To describe then the probability density of $\delta\boldsymbol{\phi}$, consider that $\delta i(t)$ is assumed to be a white noise, i.e., to have a distribution with spherical symmetry. Since FTs are orthogonal transformations, the FT of $\delta i(t)$ will be again white[1] with the same variance σ^2.

[1]We recall that it is the *power spectrum* of white noise that is flat.

Assume then for simplicity that $\delta i(t)$ is zero-mean Gaussian, so that

$$\boldsymbol{\phi}^m \sim \begin{cases} \mathcal{N}\left(\boldsymbol{\phi}^h, \sigma^2 I_2\right) & \text{if } \mathcal{H}_0 \\ \mathcal{N}\left(\boldsymbol{\phi}^f, \sigma^2 I_2\right) & \text{if } \mathcal{H}_1 \end{cases} \tag{27}$$

with I_2 the 2×2 identity matrix. The probability of type I errors (i.e., choosing $\mathcal{H}_1$ when $\mathcal{H}_0$ is true) is then

$$\mathbb{P}\left[g\left(i_{as}^m\right) = \mathcal{H}_1 \text{ under } H_0\right].$$

Due to symmetry reasons, the probability of type II errors (i.e., choosing $\mathcal{H}_0$ when $\mathcal{H}_1$ is true) is equal to the probability of type I errors.

Proposition 2 Letting $\xi \sim \mathcal{N}(0,1)$, and under the assumptions above,

$$\mathbb{P}\left[g\left(i_{as}^m\right) = \mathcal{H}_1 \text{ under } H_0\right] = \mathbb{P}\left[\xi > \frac{m}{2\sigma}\right]. \tag{28}$$

Proof Consider that

$$\mathbb{P}\left[g\left(i_{as}^m\right) = \mathcal{H}_1 \text{ under } H_0\right] = \mathbb{P}\left[w^T\left(\boldsymbol{\phi}^h + \delta\boldsymbol{\phi}\right) - b < 0\right].$$

Since $\boldsymbol{\phi}^m$ is a support vector for problem (18), i.e., $w^T\boldsymbol{\phi}^h - b = 1$, the faulty condition reduces to $w^T\delta\boldsymbol{\phi} < -1$. Define then

$$u = \begin{bmatrix} u_1 \\ u_2 \end{bmatrix} := \frac{\boldsymbol{\phi}^h - \boldsymbol{\phi}^f}{\|\boldsymbol{\phi}^h - \boldsymbol{\phi}^f\|} \tag{29}$$

and notice that $u_1^2 + u_2^2 = 1$. Exploiting then the definition of the margin m in (23), the faulty condition reduces to $u_1\delta_1 + u_2\delta_2 < -\frac{m}{w}$, where δ_1 and δ_2 are the two components of $\delta\boldsymbol{\phi}$. The proposition follows then from the fact that δ_1 and δ_2 are independent, and thus that

$$\xi := \frac{u_1\delta_1 + u_2\delta_2}{\sigma} \sim \mathcal{N}(0,1) \tag{30}$$

and the fact that $\mathbb{P}\left[\xi < -\frac{m}{2\sigma}\right] = \mathbb{P}\left[\xi > \frac{m}{2\sigma}\right]$. ■

Summarizing, (28) can be seen as a map from the quality of the DAQ measurement system (σ) and the difference between theoretical healthy and faulty operations (m) to the probability of committing type I or II errors. Graphically, this map is given in Figure 4.

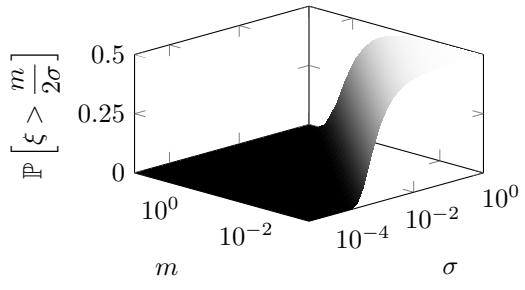

Figure 4. Dependency of (28), i.e., the probability of committing errors of type I or II, on the measurements quality index σ^2 and on the difference between the theoretical healthy and faulty operations index m.

C. Interpreting (24) as a test between two simple hypotheses

It is immediate to interpret (24) using classical statistical hypothesis testing frameworks. More specifically, the test is to check hypotheses on the unknown mean of a Gaussian with given variance (cf. (27)), where the hypotheses are simple (i.e., not sets of values but rather two simple vectors, namely $\boldsymbol{\phi}^h$ and $\boldsymbol{\phi}^f$).

Rewriting then the statistical test (24) as

$$g\left(i_{as}^m\right) = \begin{cases} \mathcal{H}_0 & \text{if } \left\|\boldsymbol{\phi}^m - \boldsymbol{\phi}^h\right\|^2 > \left\|\boldsymbol{\phi}^m - \boldsymbol{\phi}^f\right\|^2, \\ \mathcal{H}_1 & \text{otherwise,} \end{cases} \tag{31}$$

one recognizes that the condition for selecting $\mathcal{H}_0$ is

$$\frac{\exp\left(\sigma^{-2}\left\|\boldsymbol{\phi}^m - \boldsymbol{\phi}^h\right\|^2\right)}{\exp\left(\sigma^{-2}\left\|\boldsymbol{\phi}^m - \boldsymbol{\phi}^f\right\|^2\right)} > 1 \tag{32}$$

i.e., a likelihood ratio. Thus, thanks to the Neyman-Pearson Lemma [35, Thm. 4.2.1], the test $g(\cdot)$ is Most Powerful (MP) given the level of errors of type I (i.e., given the size) (28).

This thus motivates why detecting broken bars from motor current signatures using SVC concepts is, under these assumptions on the measurement noise, statistically optimal.

XII. Experimental Results

In this section we evaluate the proposed methodology in a particular real case by means of an experimental test bed that is designed for detecting broken bars in squirrel cage induction motors.

The experimental setup, depicted in Figure 5, consists of a three phase induction motor, a DC generator that works as a load for the motor, and a DAQ instrumentation that measures and collects (with a 5-kHz sampling frequency) the stator currents $i_{as}^m(t)$, $i_{bs}^m(t)$, and $i_{cs}^m(t)$, and the stator voltages $v_{as}^m(t)$, $v_{bs}^m(t)$, and $v_{cs}^m(t)$.

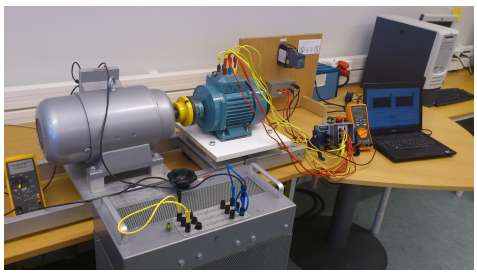

Figure 5. Photo of the experimental setup used for evaluating our broken bar fault detection methodology. The induction motor used in our experiments is on the right; the DC generator used as a load is on the left.

Our fault detection procedure starts with constructing the SVC test by using the nominal parameters of the considered IM available in Table I. This information is used to build the circuits represented in Figures 2 and 3 in Section IV. After building the circuits, one computes the currents $i_{as}^h(t)$ and $i_{as}^f(t)$ (Section V), then their spectra (shown for our experiments in Figure 6), and eventually the features $\boldsymbol{\phi}^h$ and $\boldsymbol{\phi}^f$ through (15) and (11) (Section VII). This leads to obtain a classifier of the form (24) without having exploited at all measured signals.

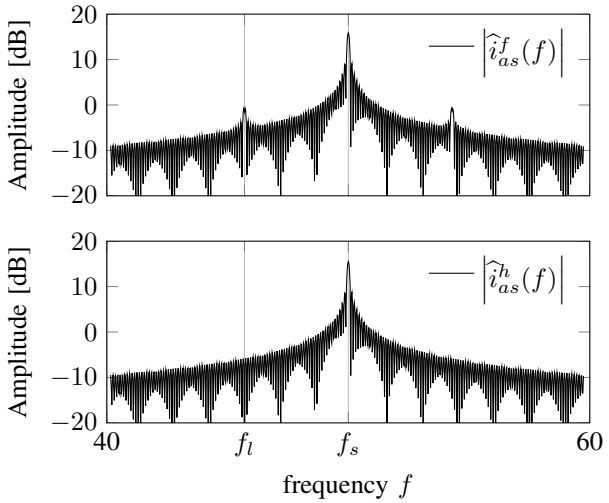

Figure 6. Amplitude of the Fourier Transforms (FTs) of the theoretical windowed stator currents under faulty (top panel) and healthy (bottom panel) conditions. It can be noticed that the two spectra markedly differ around the lower and upper sidebands.

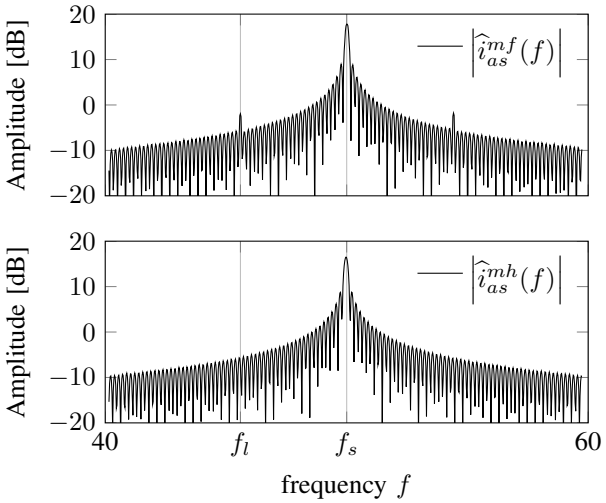

Figure 8. Amplitude of the Fourier Transforms (FTs) of the measured windowed stator currents under faulty (top panel) and healthy (bottom panel) conditions. Again, the two spectra markedly differ around the lower and upper sidebands. The measured spectra, moreover, reproduce the theoretical ones plotted in Figure 6, and this is an indication that the theoretical models reproduce sufficiently accurately the measured reality.

To test the classifier (24) we then collect data corresponding to the following two situations:

1) a healthy and properly working motor under full load conditions with the specifications given in Table I. We denote the corresponding stator current signal with $i^{mh}_{as}(t)$;
2) the same motor under full load and faulty conditions created by deliberately drilling a rotor's bar (see Figure 7). We denote the corresponding stator current signal with $i^{mf}_{as}(t)$;

The spectra of the measured signals $i^{mh}_{as}(t)$ and $i^{mf}_{as}(t)$ are then represented in Figure 8.

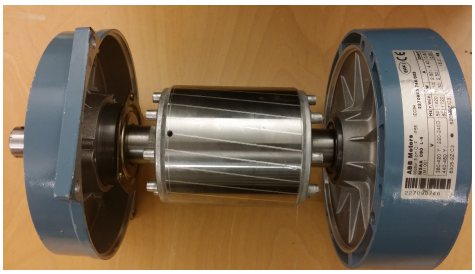

Figure 7. Detail of the motor used in our experiments: the broken rotor bar fault has been artificially produced by drilling a hole in the squirrel cage.

Table I
NOMINAL CHARACTERISTICS OF THE THREE-PHASE INDUCTION MOTOR USED IN OUR EXPERIMENTS.

parameter	*description*	*nominal value*
p	Pole Numbers	4
V_m	Rated Voltage	537 V
f_s	Frequency	50 Hz
	Rated Power	1.1 kW
I_m	Rated current, Y Connection	3.5 A
r_s	Stator resistance	4.8 Ohm
r_r	Rotor resistance	5 Ohm
x_s	Stator inductance	48 mH
x_r	Rotor inductance	48 mH
x_m	Mutual inductance	0.636 H

The measured features to be used in the SVC classifiers are then the fundamental harmonic, located at f_s, and its left sideband, located at f_l. As it can be observed from Figure 9, the proposed model based SVC test accurately discriminates the broken and healthy motors used in our experimental results.

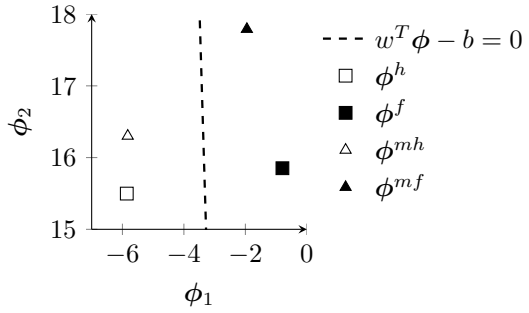

Figure 9. Overall assessment of the SVC procedure: the squares represent the theoretically derived features, from which one computes the separating hyperplane $w^T\phi - b = 0$. The triangles instead represent the measured features, obtained from testing the real device described above. The features with white interior represent healthy motors, while the ones with black interior represent faulty motors.

XIII. CONCLUSIONS

We presented a model based Support Vector Classification (SVC) method for detecting broken rotor bars in three phase asynchronous motors. We consider features that are extracted from the spectral analysis of the stator currents (more specifically the amplitude of the fundamental and the left sideband harmonics) at full load conditions.

We investigated what are the capabilities of using theoretically derived SVC rules, driven by our interests in the practical cases where one needs to construct faults detectors in the

situation where measurements from both healthy and faulty systems are simultaneously not available.

The main messages brought by this manuscript are that: *a)* using theoretically derived SVCs can be meaningful in practical cases: the method has indeed been experimentally evaluated, and has been able to detect the fault occurrence in the examined case; *b)* SVC is a statistically meaningful approach when considering Motor Current Signature Analysis (MCSA). Indeed we proved how, under mild conditions on the measurement noise, using SVC methods is statistically optimal under classical hypothesis testing frameworks.

The methodology is nonetheless still in its infancy: future works need to address specially the robustness to load variations, changing operating conditions (indeed thermal effects make the parameters such as resistances and inductances vary), and in general the effects of model uncertainties.

REFERENCES

[1] H. Henao, G. A. Capolino, M. Fernandez-Cabanas, F. Filippetti, C. Bruzzese, E. Strangas, R. Pusca, J. Estima, M. Riera-Guasp, and S. Hedayati-Kia, "Trends in Fault Diagnosis for Electrical Machines: A Review of Diagnostic Techniques," *IEEE Industrial Electronics Magazine*, vol. 8, no. 8, pp. 31–42, 2014.

[2] S. Nandi, H. Toliyat, S. Nandi, and H. Toliyat, "Condition monitoring and fault diagnosis of electrical machines-a review," *IEEE Transactions on Energy Conversion*, vol. 20, no. 4, pp. 719–729, 2005.

[3] P. Santos and T. Lubiny, "A Simplified Induction Machine Model to Study Rotor Broken Bar Effects and for Detection," *European Transactions On Electrical Power*, vol. 20, p. 611, 2010.

[4] G. G. Acosta, C. J. Verucchi, and E. R. Gelso, "A current monitoring system for diagnosing electrical failures in induction motors," *Mechanical Systems and Signal Processing*, vol. 20, no. 4, pp. 953–965, 2004.

[5] I. Y. Anel, I. Azenol, and M. E. H. Benbouzid, "Induction Motors Bearing Failures Detection and Diagnosis Using a RBF ANN Park Pattern Based Method," *International Electric Machines and Drives Conference*, pp. 1073–1078, 2007.

[6] P. Sushma, B.L.R. Samaga, and K. Vittal, "DQ modeling of induction motor for virtual flux measurement," *9th International Power and Energy Conference, IPEC*, pp. 903–908, 2010.

[7] S. J. Arif, M. Imdadullah, and S. J. Asghar, "Rotating magnetic field based instantaneous angular speed measurement of low speed rotating machines," *International conference on multimedia, signal processing and communication technologies*, pp. 252–255, 2011.

[8] K. Bacha, H. Henaob, M. Gossa, and G. Capolino, "Induction machine fault detection using stray flux emf measurement and neural network based decision," *European Transactions On Electrical Power*, vol. 78, pp. 1247–1255, 2008.

[9] W. Thomason and P. Orpin, "Current and vibration monitoring for fault diagnosis and root cause analysis of induction motor drives," *Proceedings of the Thirty-First Turbomachinery Symposium*, 2002.

[10] Z. Gao and X. Dai, "From model, signal to knowledge: a data-driven perspective of fault detection and diagnosis," *IEEE Transactions on Industrial Informatics*, vol. 9, no. 4, pp. 2226–2238, 2013.

[11] E. Cabal-Yepez, A. Garcia-Ramirez, R. Romero-Troncoso, A. Garcia-Perez, and R. Osornio-Rios, "Reconfigurable Monitoring System for Time-Frequency Analysis on Industrial Equipment Through STFT and DWT," *IEEE Transactions on Industrial Informatics*, vol. 9, no. 2, pp. 760–771, 2013.

[12] A. Da Silva, N. Demerdash, and R. J. Povinelli, "Rotor Bar Fault Monitoring Method Based on Analysis of Air-Gap Torques of Induction Motors," *IEEE Transactions on Industrial Informatics*, vol. 9, no. 4, pp. 2274–2283, 2013.

[13] J. Antonino Daviu, S. Aviyente, E. G. Strangas, and M. Riera-Guasp, "Scale Invariant Feature Extraction Algorithm for the Automatic Diagnosis of Rotor Asymmetries in Induction Motors," *IEEE Transactions on Industrial Informatics*, vol. 9, no. 1, pp. 100–108, Feb. 2013.

[14] J. Faiz, V. Ghorbanian, and B. Ebrahimi, "EMD-Based Analysis of Industrial Induction Motors with Broken Rotor Bar for Identification of Operating Point at Different Supply Modes," *IEEE Transactions on Industrial Informatics*, vol. 10, no. 2, pp. 957–966, 2014.

[15] A. Johansson, M. Bask, and T. Norlander, "Dynamic threshold generators for robust fault detection in linear systems with parameter uncertainty," *Automatica*, vol. 42, no. 7, pp. 1095–1106, July 2006.

[16] S. Bachir, S. Tnani, J.-C. Trigeassou, and G. Champenois, "Diagnosis by parameter estimation of stator and rotor faults occurring in induction machines," *IEEE Transactions on Industrial Electronics*, vol. 53, no. 3, pp. 963–973, June 2006.

[17] K. Kim and a.G. Parlos, "Model-Based Fault Diagnosis of Induction Motors Using Non-Stationary Signal Segmentation," *Mechanical Systems and Signal Processing*, vol. 16, no. 2-3, pp. 223–253, Mar. 2002.

[18] V. N. Vapnik, *Statistical learning theory*. New York: Wiley, 1998.

[19] A. Widodo and B.-S. Yang, "Support vector machine in machine condition monitoring and fault diagnosis," *Mechanical Systems and Signal Processing*, vol. 21, no. 6, pp. 2560–2574, Aug. 2007.

[20] L. M. R. Baccarini, V. V. Rocha e Silva, B. R. de Menezes, and W. M. Caminhas, "SVM practical industrial application for mechanical faults diagnostic," *Expert Systems with Applications*, vol. 38, no. 6, pp. 6980–6984, June 2011.

[21] H. Keskes, A. Braham, and Z. Lachiri, "Broken rotor bar diagnosis in induction machines through stationary wavelet packet transform and multiclass wavelet SVM," *Electric Power Systems Research*, vol. 97, pp. 151–157, Apr. 2013.

[22] J. Kurek and S. Osowski, "Support vector machine for fault diagnosis of the broken rotor bars of squirrel-cage induction motor," *Neural Computing and Applications*, vol. 19, no. 4, pp. 557–564, Oct. 2010.

[23] G. B. Kliman and J. Stein, "Methods of Motor Current Signature Analtysis," *Electrical Machines and Power Systems*, vol. 20, no. 5, pp. 436–474, Sept. 1992.

[24] W. T. Thomson and R. J. Gilmore, "Motor current signature analysis to detect faults in induction motor drives-fundamentals, Data interpretation, and industrial case histories," in *Proceedings of 32nd Turbomachinery Symposium*, no. 1987, 2003.

[25] E. H. M. Benbouzid, "A review of induction motors signature analysis as a medium for faults detection," *IEEE Transactions on Industrial Electronics*, vol. 47, no. 5, pp. 984–993, 2000.

[26] E. H. El Bouchikhi, V. Choqueuse, and M. Benbouzid, "Induction machine faults detection using stator current parametric spectral estimation," *Mechanical Systems and Signal Processing*, vol. 52-53, pp. 447–464, Feb. 2015.

[27] A. M. da Silva, R. J. Povinelli, and N. A. O. Demerdash, "Induction Machine Broken Bar and Stator Short-Circuit Fault Diagnostics Based on Three-Phase Stator Current Envelopes," *IEEE Transactions On Industrial Electronics*, vol. 55, no. 3, pp. 1310–1318, Mar. 2008.

[28] Motor Reliability Working Group, W. Group, P. Systems, R. Subcommittee, E. Committee, I. Industry, and A. Society, "Report of Large Motor Reliability Survey of Industrial and Commercial Installations, Part II," *IEEE Transactions on Industry Applications*, vol. IA-21, no. 4, pp. 853–864, 1985.

[29] Motor Reliability Working Group, "Report of Large Motor Reliability Survey of Industrial and Commercial Installations: Part III," *IEEE Transactions on Industry Applications*, vol. IA-23, no. 1, pp. 153–158, Jan. 1987.

[30] A. Bellini, F. Filippetti, G. Franceschini, C. Tassoni, and G. B. Kliman, "Quantitative evaluation of induction motor broken bars by means of electrical signature analysis," *IEEE Transactions on Industry Applications*, vol. 37, no. 5, pp. 1248–1255, 2001.

[31] F. Filippetti and M. Martelli, "Development of expert system knowledge base to on-line diagnosis of rotor electrical faults of induction motors," in *Conference Record of the IEEE Industry Applications Society Annual Meeting*, 1992.

[32] S. Chen and R. Zivanovic, "Modelling and simulation of stator and rotor fault conditions in induction machines for testing fault diagnostic techniques," *European Transactions On Electrical Power*, vol. 20, pp. 611–629, Apr. 2009.

[33] M. O. Mustafa, G. Nikolakopoulos, and T. Gustafsson, "Broken Bars Fault Diagnosis Based on Uncertainty Bounds Violation for Three Phase Induction Motors," *International Transactions on Electrical Energy Systems*, 2013.

[34] F. Gu, T. Wang, A. Alwodai, X. Tian, Y. Shao, and A. D. Ball, "A new method of accurate broken rotor bar diagnosis based on modulation signal bispectrum analysis of motor current signals," *Mechanical Systems and Signal Processing*, vol. 50-51, pp. 400–413, 2015.

[35] M. Basseville and I. Nikiforov, *Detection of Abrupt Changes - Theory and Application*. Prentice Hall, 1993.